

2. Laquay N, Prieur S, Greff B, Meyer P, Orliaguet G. Propofol infusion syndrome. *Ann Fr Anesth Reanim.* 2010;29:377–386.
3. Fodale V, La Monaca E. Propofol infusion syndrome: an overview of a perplexing disease. *Drug Saf.* 2008;31:293–303.
4. Mirrakhimov AE, Voore P, Halytskyy O, Khan M, Ali AM. Propofol infusion syndrome in adults: a clinical update. *Crit Care Res Pract.* 2015. <http://dx.doi.org/10.1155/2015/260385>.
5. Dengler B, Garvin R, Seifi A. Can therapeutic hypothermia trigger propofol-related infusion syndrome? *J Crit Care.* 2015;30:823–824.

<http://dx.doi.org/10.1016/j.rec.2017.05.017>
1885-5857/

© 2017 Sociedad Española de Cardiología. Published by Elsevier España, S.L.U. All rights reserved.

Patient-specific 3D-printed Cardiac Model for Percutaneous Left Atrial Appendage Occlusion



Impresión 3D de modelos cardíacos personalizados para el cierre percutáneo de la orejuela izquierda

To the Editor,

Generally, percutaneous left atrial appendage (LAA) occlusion procedures are guided by 2-dimensional (2D) transesophageal echocardiography (TEE) and fluoroscopy. However, correct sizing of the required devices remains a challenging phase of the process. Furthermore, any advances able to minimize manipula-

tion within the LAA and ease the implantation process would be welcomed.¹

Patient-specific 3-dimensional (3D) heart models generated via 3D printing enable life-like replicas of image-based human anatomy, such as that obtained through multislice computed tomography, magnetic resonance imaging, and 3D echocardiography. This new technology impacts many medical specialties and has received increasing attention in the literature.^{2,3} Physical models of LAA occlusion are particularly relevant, because the anatomy is complex, and even if cutting-edge imaging is applied, gauging the interactions between the device and appendage is difficult.⁴

Our preliminary experience with patient-specific 3D-printed models of the LAA is presented herein, with the following

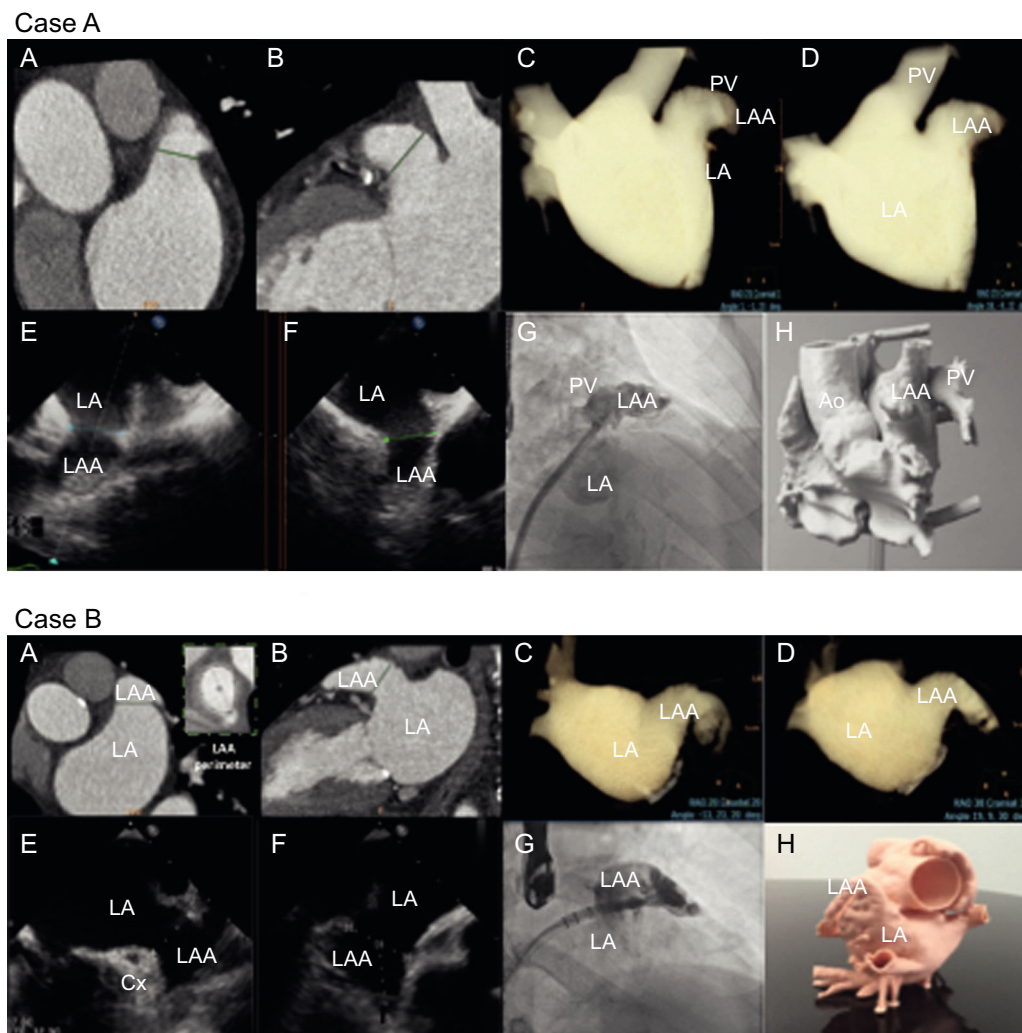


Figure 1. Multimodal imaging of LAA for cases A and B). A, B: cardiac measurements via computed tomography. C, D: computed tomography rendering of left atrial volume in working projections. E, F: transesophageal echocardiographic views (45° and 135°) showing landing zone. G: right anterior oblique cranial fluoroscopic projections; and H: 3-dimensional printed model. Ao, aorta; Cx, circumflex; LA, left atrium; LAA, left atrial appendage; PV, pulmonary vein.

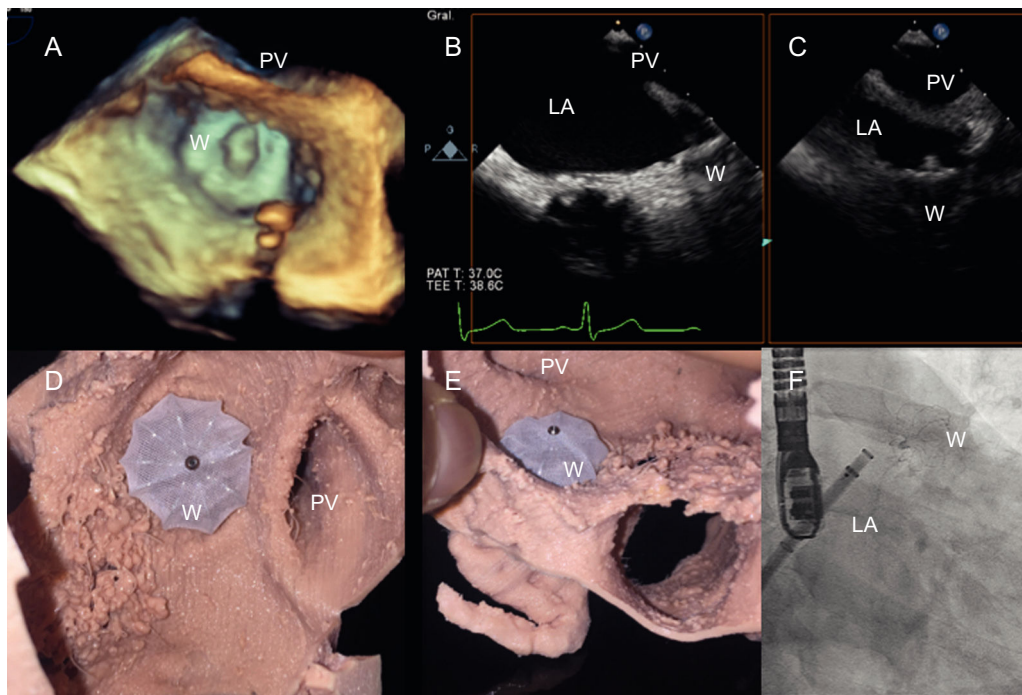


Figure 2. *Ex vivo* rehearsal phase and final outcome of left atrial appendage closure. A: 3-dimensional transesophageal echocardiogram. B, C: 2-dimensional transesophageal echocardiogram. D, E: 3-dimensional printed model; and F: fluoroscopic right anterior oblique cranial projection. W, Watchman device; LA, left atrium; PV, pulmonary vein.

objectives: *a*) to better appreciate LAA anatomy, location, and relationships; *b*) to aid in device sizing; and *c*) to optimize planning of LAA occlusion.

Ten patients with atrial fibrillation and with clinical indications for LAA closure were included in this initial analysis. In these 10 patients, multislice computed tomography images of the heart were segmented (ITK-SNAP freeware) and 3D meshes were created for 3D printing (220 °C, 10 mm/s, 0.1 mm layer height, 0.8 mm wall thickness) by an established method³ (Figure 1).

Each LAA model required 500€ to produce and 24 to 48 hours to complete. The printed models then served in the training/rehearsal phase. Expired LAA closure devices were deployed at this juncture to determine the following: *a*) ideal device, *b*) proper device size, and *c*) various orientations within the LAA conducive to either the success or failure of percutaneous closure. Device suitability was based on visually assessed anatomic deformation (in a specified LAA backdrop) and the feasibility of engagement within the flexible 3D atrial model (Figure 2).

As we observed, mean LAA diameters showed high degrees of correlation in imaging comparisons: computed tomography vs 2D-TEE (Pearson correlation coefficient [*r*], 0.98; *P* < .0001), fluoroscopy vs 2D-TTE (*r*, 0.92; *P* < .0001), and computed tomography vs fluoroscopy (*r*, 0.96; *P* < .0001). However, the mean values generated via 2D-TEE (21.9 ± 3.8 mm) and fluoroscopy (22.2 ± 3.7 mm) were significantly lower than those registered by computed tomography (23.1 ± 3.8 mm) (*P* < .001 and *P* = .02, respectively). All 3D printing-derived device sizes nonetheless fully reflected those actually deployed, with no circumferential leakage. No adverse events were recorded at 30-day follow-up monitoring.

Of note, Budge et al.¹ have reported a similar correlation between LAA measurements done by multislice computed

tomography and by 2D-TEE. In addition, Otton et al.⁵ have shown that accurate approximations of device size (underestimated using TEE) are feasible with 3D-printed models. Finally, 2 instances of accurately sized and optimally implanted devices, based on a 3D-printed model (TEE and fluoroscopy estimates again low), have been documented by Pellegrino et al.⁶

From our perspective, the development of patient-specific 3D-printed physical models holds a wealth of promise in terms of proper device sizing under difficult circumstances, insights into LAA anatomic interrelationships, and viable device-specific technical strategies. There is also a potential to educate professionals accordingly, clarifying the aims and limitations of LAA occlusion. On the other hand, more clinical studies are needed to validate these uses, and logistics are of some concern. Although 3D heart models and 3D printing technology are now more widely available and more affordable, expenditures of time, money, and effort are still barriers to daily clinical use.

Acknowledgments

We are grateful to Drs Israel Valverde, Xavier Freixa and Oscar Alcade for their willing collaboration and review of this study.

FUNDING

This study received financial support from St Jude Medical, Inc (Minnesota, US). The sponsor had no role in designing the study, data collection, data analysis, data interpretation, or writing of the report. This research was cofinanced by Institute of Health Carlos III – FIS research grant number PI14/00180 from the Spanish Ministry of Science and Innovation.

CONFLICTS OF INTEREST

I. Cruz-González is a clinical proctor for St Jude Medical and for Boston Scientific.

Beatriz Vaquerizo,^{a,*} Carmen Escabias,^b Daniela Dubois,^a Gorka Gómez,^c Manuel Barreiro-Pérez,^d and Ignacio Cruz-González^d

^aUnidad de Cardiología Intervencionista, Servicio de Cardiología, Hospital del Mar, Universidad Autónoma de Barcelona, Barcelona, Spain

^bUnidad de Cardiología Pediátrica, Hospital Virgen del Rocío, Sevilla, Spain

^cGrupo de Innovación Tecnológica, Hospital Virgen del Rocío, Sevilla, Spain

^dServicio de Cardiología, Hospital Universitario de Salamanca, IBSAL, Salamanca, Spain

* Corresponding author:

E-mail address: beavaquerizo@yahoo.es (B. Vaquerizo).

Available online 24 June 2017

REFERENCES

1. Budge LP, Shaffer KM, Moorman JR, Lake DE, Ferguson JD, Mangrum JM. Analysis of in vivo left atrial appendage morphology in patients with atrial fibrillation: a direct comparison of transesophageal echocardiography, planar cardiac CT, and segmented three-dimensional cardiac CT. *J Interv Cardiac Electrophysiol.* 2008;23:87–93.
2. Vaquerizo B, Theriault-Lauzier P, Piazza N. Percutaneous transcatheter mitral valve replacement: patient-specific three-dimensional computer-based heart model and prototyping. *Rev Esp Cardiol.* 2015;68:1165–1173.
3. Valverde I. Three-dimensional printed cardiac models: applications in the field of medical education, cardiovascular surgery, and structural heart interventions. *Rev Esp Cardiol.* 2017;70:282–291.
4. Pracon R, Grygoruk R, Dzielinska Z, et al. Percutaneous occlusion of the left atrial appendage with complex anatomy facilitated with 3D-printed model of the heart. *EuroIntervention.* 2016;12:927.
5. Otton JM, Spina R, Sulas R, et al. Left atrial appendage closure guided by personalized 3D-printed cardiac reconstruction. *JACC Cardiovasc Interv.* 2015;8:1004–1006.
6. Pellegrino PL, Fassini G, Di Biase M, Tondo C. Left atrial appendage closure guided by 3d printed cardiac reconstruction: emerging directions and future trends. *J Cardiovasc Electrophysiol.* 2016;27:768–771.

<http://dx.doi.org/10.1016/j.rec.2017.05.028>
1885-5857/

© 2017 Sociedad Española de Cardiología. Published by Elsevier España, S.L.U. All rights reserved.

Malignant Pericardial Effusion as a Presentation of AIDS: The Role of Flow Cytometry in Early Diagnosis



Derrame pericárdico maligno como presentación de sida: papel de la citometría de flujo en el diagnóstico precoz

To the Editor,

We present the case of a 31-year-old man with no medical history of interest, who presented to the emergency room of a regional hospital with a 1-week history of asthenia and general malaise, associated with diffuse abdominal discomfort, dry cough, and predominantly nocturnal sweating. Physical examination detected hypophonesis in both lung bases and an increase in jugular venous pressure. Laboratory analyses showed bicytopenia (leukocytes, 3800/μL; hemoglobin, 10.7 g/dL) and C-reactive protein concentration at 5.90 mg/dL (upper normal

limit, 0.5 mg/dL). Chest radiography depicted cardiomegaly and bilateral pleural effusion. As part of the diagnostic study, transthoracic echocardiography was requested. The examination showed severe pericardial effusion with echocardiographic evidence of tamponade (Figure), which prompted his transferal to our center.

The patient was admitted to the cardiac critical care unit, where pericardiocentesis was successfully carried out, yielding 1350 mL of serohematic fluid. On biochemical analysis, the fluid was identified as an exudate (proteins, 3.1 g/dL; fluid/plasma protein ratio, 0.57; lactate dehydrogenase, 1295 U/L), with an adenosine deaminase level of 26.4 U/L and abundant red blood cells. Cytology showed atypical lymphocytes with an immunoblastic appearance, prompting a request for flow cytometry study. Cytometry identified 54% of hematopoietic cells (CD45), which were large (elevated SSC) and negative for B-cell antigens (CD19) and T-cell antigens (CD3). They were, however, positive for activation antigens, such as HLA-DR and CD30, and for plasma cell markers,

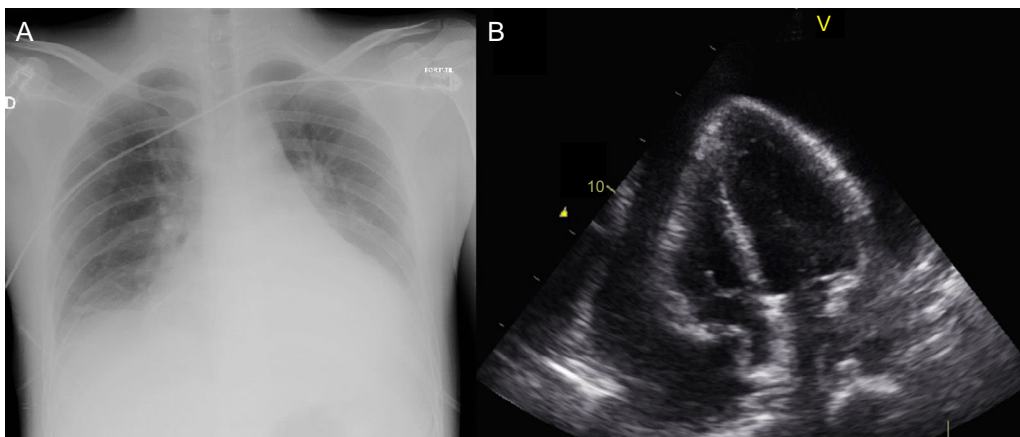


Figure. A, Chest radiograph showing overall cardiomegaly and bilateral pleural effusion. B, Apical 4-chamber view obtained with transthoracic echocardiography, showing a severe pericardial effusion with diastolic collapse of the right atrium.